Acta Oceanol. Sin., 2015, Vol. 34, No. 1, P. 3–10
DOI: 10.1007/s13131-015-0590-2
http://www.hyxb.org.cn
E-mail: hyxbe@263.net

Winter coastal upwelling off northwest Borneo in the South China Sea

YAN Yunwei[1, 2], LING Zheng[2]*, CHEN Changlin[2]

[1] College of Physical and Environmental Oceanography, Ocean University of China, Qingdao 266100, China
[2] State Key Laboratory of Satellite Ocean Environment Dynamics, Second Institute of Oceanography, State Oceanic Administration, Hangzhou 310012, China

Received 3 March 2014; accepted 18 April 2014

Abstract

Winter coastal upwelling off northwest Borneo in the South China Sea (SCS) is investigated by using satellite data, climatological temperature and salinity fields and reanalysis data. The upwelling forms in December, matures in January, starts to decay in February and almost disappears in March. Both Ekman transport induced by the alongshore winter monsoon and Ekman pumping due to orographic wind stress curl are favorable for the upwelling. Transport estimates demonstrate that the month-to-month variability of Ekman transport and Ekman pumping are both consistent with that of winter coastal upwelling, but Ekman transport is two times larger than Ekman pumping in January and February. Under the influence of El Niño-Southern Oscillation (ENSO), the upwelling shows remarkable interannual variability: during winter of El Niño (La Niña) years, an anticyclonic (a cyclonic) wind anomaly is established in the SCS, which behaves a northeasterly (southwesterly) anomaly and a positive (negative) wind stress curl anomaly off the northwest Borneo coast, enhancing (reducing) the upwelling and causing anomalous surface cooling (warming) and higher (lower) chlorophyll concentration. The sea surface temperature anomaly (SSTA) associated with ENSO off the northwest Borneo coast has an opposite phase to that off southeast Vietnam, resulting in a SSTA seesaw pattern in the southern SCS in winter.

Key words: coastal upwelling, northwest Borneo, South China Sea, Ekman transport, Ekman pumping, interannual variability

Citation: Yan Yunwei, Ling Zheng, Chen Changlin. 2015. Winter coastal upwelling off northwest Borneo in the South China Sea. Acta Oceanologica Sinica, 34(1): 3–10, doi: 10.1007/s13131-015-0590-2

1 Introduction

Coastal upwelling, as the best known type of upwelling, occurs near the coast as a result of Ekman transport: uniform alongshore winds push water offshore due to the Earth's rotation. To compensate for the loss of mass near the coast, cooler and nutrient-rich water is brought towards the sea surface. The nutrient-rich upwelled water stimulates the growth of primacy producers such as phytoplankton, resulting in high levels of primary productivity and fishery production. Thus coastal upwelling has significant impacts on ecosystem and fishery (Barth et al., 2007).

Besides Ekman transport, Ekman pumping induced by wind stress curl would significantly enhance local upwelling (Enriquez and Friehe, 1995; Pickett and Paduan, 2003; Castelao and Barth, 2006). During the process of Ekman pumping, wind stress curl generates divergence, forcing an upward water movement. Compared with Ekman transport, Ekman pumping makes an equal or even greater contribution to upwelling in some regions (Pickett and Paduan, 2003; Castelao and Barth, 2006; Croquette et al., 2007; Jing et al., 2009).

Borneo is the third largest island in the world, which is surrounded by the South China Sea (SCS) to the northwest, the Balabac Strait to the north and the Sulu Sea to the northeast (Fig. 1a). North-south oriented mountain ranges are located in the center of Borneo and the highest point is Mount Kinabalu with an elevation of 4095 m. In winter (winter refers to January, February and March in this study), the northeasterly monsoon prevails off northwest Borneo and blows nearly along the northwest coastline (Fig. 1a). Due to orographic blockage of the mountains, a wind jet with positive wind stress curl forms off the northwest Borneo coast (Figs 1a and b). Both Ekman transport induced by the alongshore winter monsoon and Ekman pumping due to the positive wind stress curl are favorable for winter coastal upwelling off northwest Borneo.

Studies on winter coastal upwelling off northwest Borneo are few, and they focused on upwelling ecosystem: phytoplankton and algal blooms were found here as a result of coastal upwelling associated with the northeasterly winter monsoon (Isoguchi et al., 2005; Knee et al., 2006; Wang et al., 2008). So far, spatial-temporal characteristics of the upwelling and the roles of Ekman transport and Ekman pumping in the upwelling are still not clear. In this paper, winter coastal upwelling off northwest Borneo is firstly examined using satellite data

Foundation item: The National Natural Science Foundation of China under contract No. 91128212; the National Basic Research Program of China under contract No. 2013CB430301; the National Science Fund of China for Distinguished Young Scholars (NSFDYS) under contract No. 41125019; the National Natural Science Foundation of China under contract No. 41306024; the Project of Global Change and Air-Sea Interaction under contract No. GASI-03-01-03-03; the Basic Research Program of Second Institute of Oceanography, State Oceanic Administration of China under contract No. JT1301.

*Corresponding author, E-mail: lingzheng@sio.org.cn

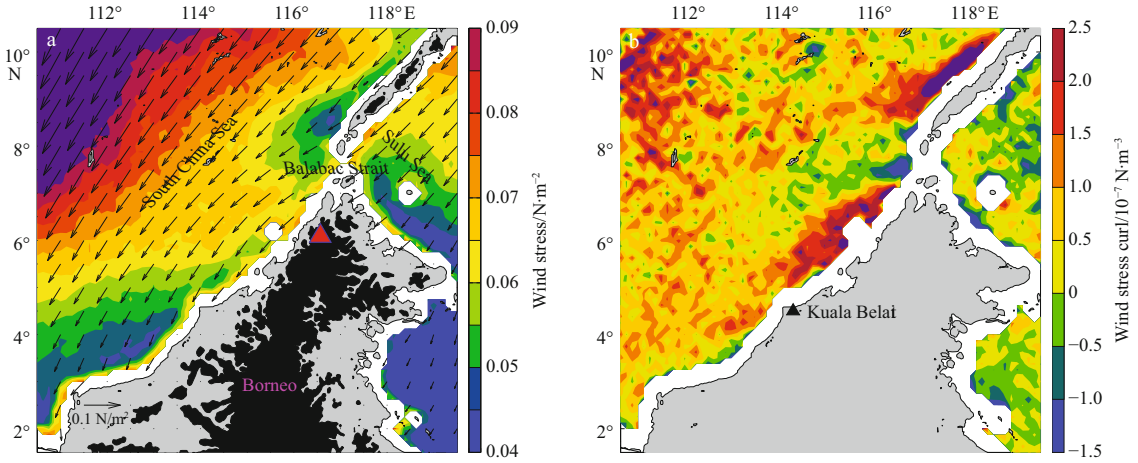

Fig. 1. QuickScat winter mean (a) wind stress (color), wind stress vector (arrow) and (b) wind stress curl. Land topography with elevations greater than 300 m is shaded in Black and the red triangle is the highest point Mount Kinabalu with an elevation of 4 095 m.

and climatological temperature and salinity fields, and then its month-to-month variation and the relative importance of Ekman transport and Ekman pumping are investigated. Lastly, the interannual variability of the upwelling is presented.

2 Data and method

Optimum interpolation (OI) of sea surface temperature (SST) analysis product (Reynolds et al., 2007), which combines advanced very high resolution radiometer (AVHRR) infrared satellite SST data with *in situ* data from ships and buoys, is used to show spatial-temporal characteristics of winter coastal upwelling. The product has a spatial grid resolution of (1/4)° and temporal resolution of 1 d. To examine the vertical structure of the upwelling, high resolution (1/4)° World Ocean Atlas (WOA01) monthly temperature and salinity climatology (Boyer et al., 2005) is also used here.

Chlorophyll-a concentration (Chl *a*) is obtained from the Moderate Resolution Imaging Spectroradiometer (MODIS) instrument aboard the Terra satellite launched in December 18, 1999. Monthly average level-3 Chl *a* with 9-km resolution is downloaded from the Ocean Color website (http://oceancolor.gsfc.nasa.gov/).

QuickScat wind stress and wind stress curl with a (1/8)° resolution derived from NOAA CoastWatch (http://coastwatch.pfeg.noaa.gov/erddap/griddap/erdQSstress1day.html) are used to estimate Ekman transport and Ekman pumping following Pickett and Paduan (2003). The Ekman transport M and Ekman pumping velocity ω are calculated as (Smith, 1968)

$$M = \frac{1}{\rho f}\vec{\tau}\times\hat{t}, \tag{1}$$

$$\omega = \frac{1}{\rho f}\nabla\times\vec{\tau}, \tag{2}$$

where $\vec{\tau}$ is wind stress vector, $\hat{t}$ is a unit vector tangent to the local coastline, ρ is the density of seawater and f is the Coriolis parameter. The Ekman pumping velocity is integrated out to 125 km offshore (approximately to where the positive wind stress curl extends) to obtain a vertical transport that could be compared with the Ekman transport calculated by Eq. (1) (Castelao and Barth, 2006).

To investigate interannual variability of winter coastal upwelling, wind speed at 10 m from 1982 to 2012 with a resolution of 0.75° derived from daily full resolution ERA-Interim, which is produced by the European Centre for Medium-Range Weather Forecasts (ECMWF) (Dee et al., 2011), is used to estimate wind stress and wind stress curl.

3 Results

3.1 *Evidences of winter coastal upwelling off northwest Borneo*

Due to upwelled cooler water and increased phytoplankton biomass, coastal upwelling can be identified by low SST and high Chl *a*. Figure 2a shows winter mean SST off northwest Borneo. The most conspicuous feature is cold water off the northwest coast with the lowest temperature about 26.9°C located nearby the coast. Meanwhile, high Chl *a* occurs in the area and its center coincides with that of the cold water (Fig. 2b). These satellite data suggest that coastal upwelling may occur off northwest Borneo in winter.

SST in winter derived from (1/4)° WOA01 data bears much resemblance with satellite data: low SST appears off the northwest Borneo coast and the minimum value is located nearby the coast (Fig. 3a). High-salinity water is also found in this region (Fig. 3b). Besides, the vertical distribution of temperature and salinity shows that the isotherms and isohalines ascend toward the northwest Borneo coast (Figs 3c and d). The climatological temperature and salinity fields confirm the occurrence of winter coastal upwelling off northwest Borneo. Furthermore, field observations capture the features of the upwelling as well (Figs 2a and d in the study of Yao et al., 2012).

3.2 *Month-to-month variation of coastal upwelling and the relative importance of Ekman transport and Ekman pumping*

Figure 4a shows month-to-month variation of SST off northwest Borneo from December to April. The cold water off the northwest coast firstly appears in December and then continues cooling until SST attains minimum values in February. After that, SST rises. Chl *a* shows similar month-to-month variability: it increases significantly in January, reaches maximum values in February and then decreases in March (Fig. 4b). The month-to-month variability of SST and Chl *a* imply that coastal upwelling

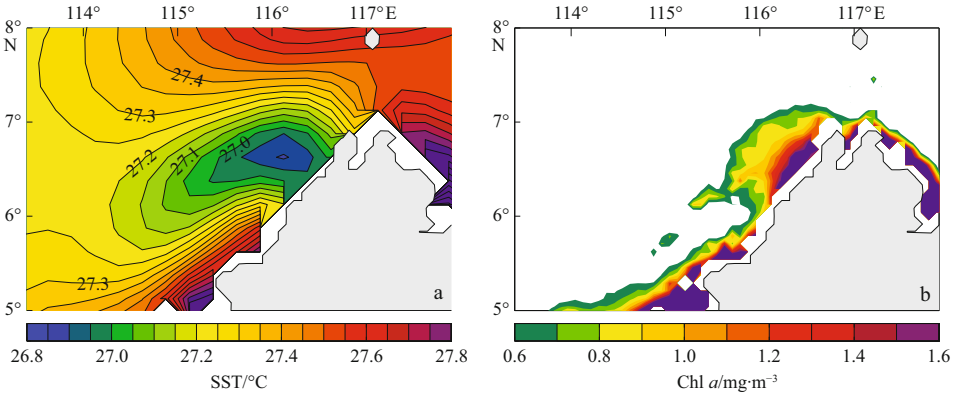

Fig. 2. Winter mean OISST (a) and MODIS Chl *a* (b) off northwest Borneo (⩾0.6 mg/m^3 are shaded).

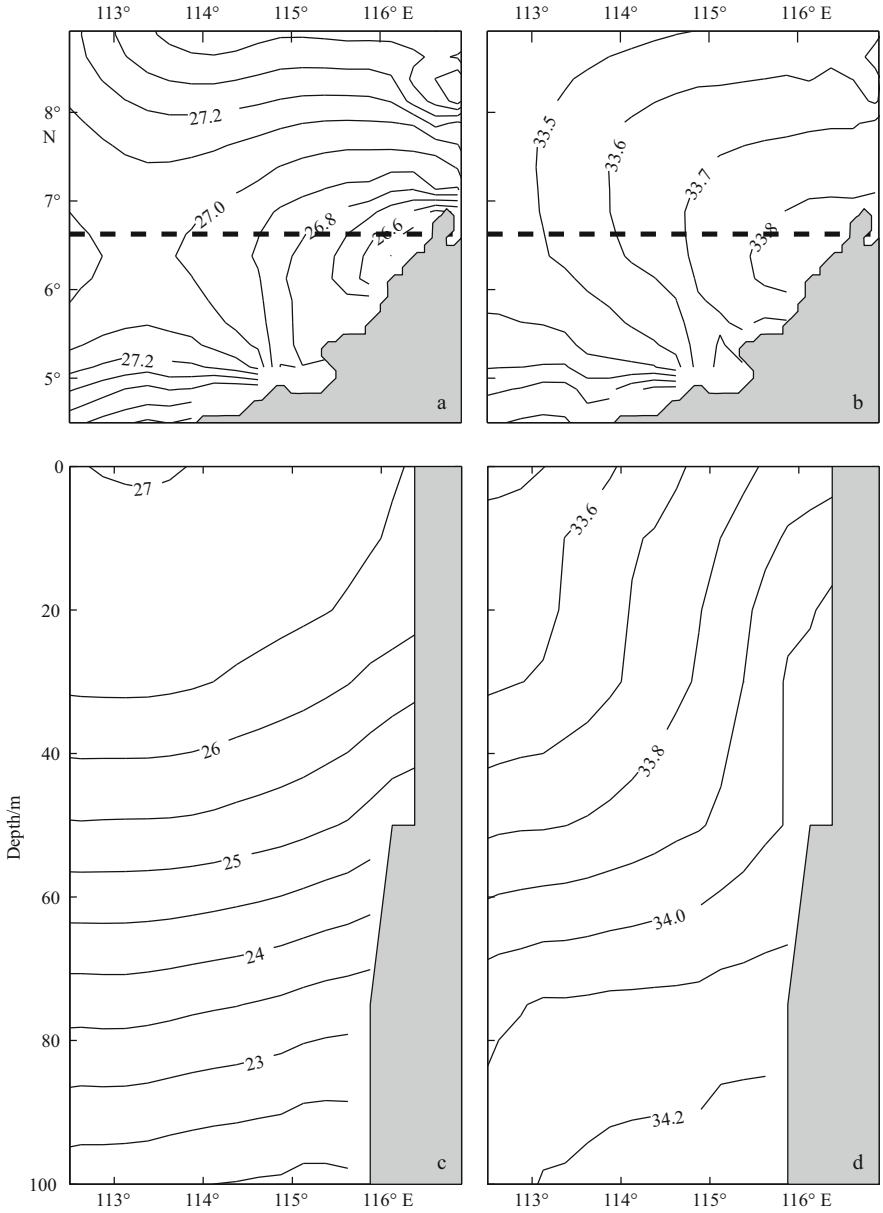

Fig. 3. The distribution of winter mean sea surface temperature (a), sea surface salinity (b), temperature along a zonal cross section (c), and salinity along a zonal cross section (d) derived from (1/4)° WOA01 data. The location of section is marked by dashed black line.

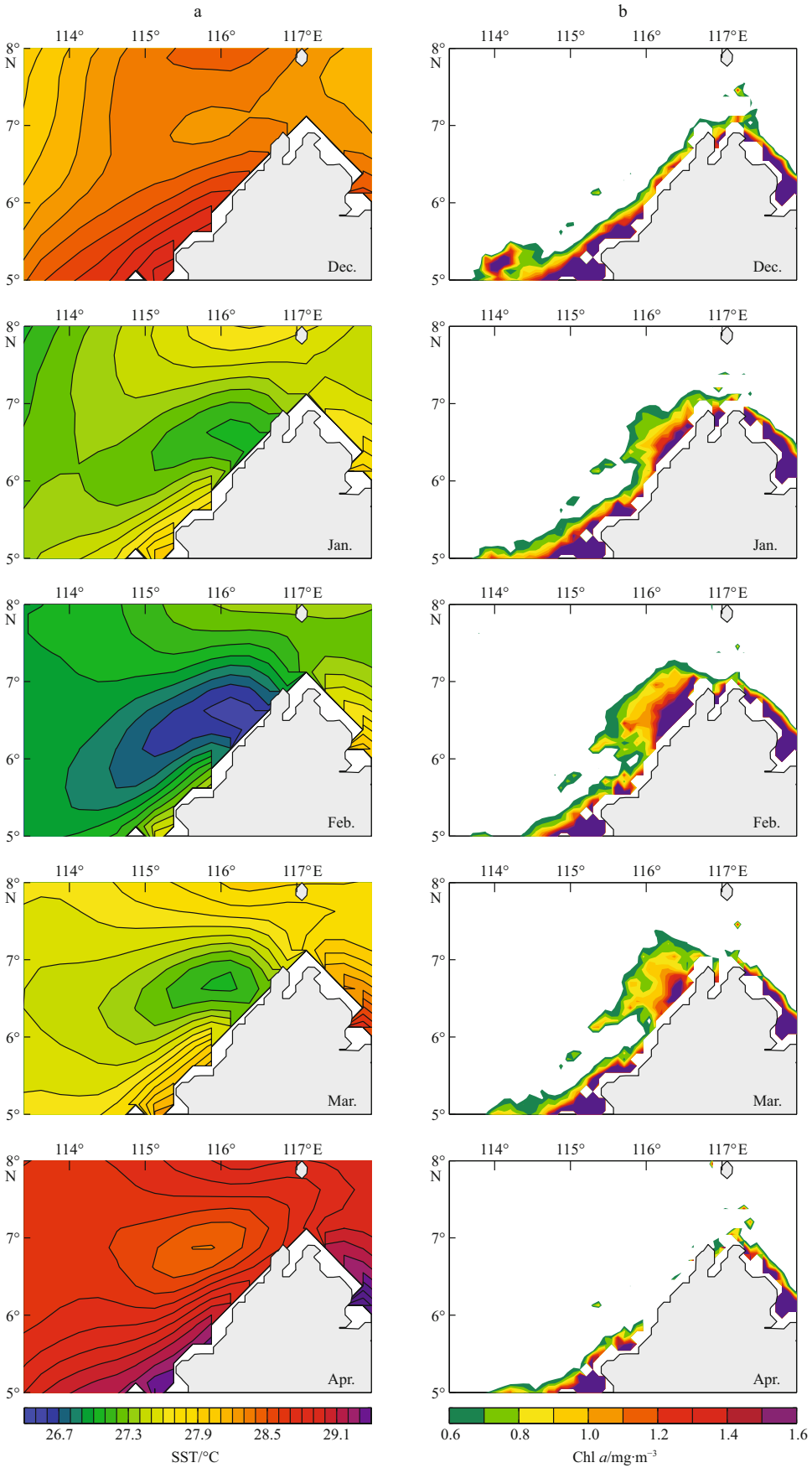

Fig. 4. Month-to-month variation of OISST (a) and MODIS Chl *a* (b) off northwest Borneo (≥0.6 mg/m^3 are shaded).

off northwest Borneo has obvious month-to-month variability as well.

Since SST and Chl *a* are the results of the cumulative effects of the upwelling, they could not be used to represent the upwelling intensity directly. To show the month-to-month variation of coastal upwelling, upwelling-induced changes in SST are used as an indicator of the upwelling intensity, which is estimated as the difference of SST tendency and SST tendency at the northern tip (marked by red line in the upper left panel of Fig. 5). Generally, SST tendency in the ocean area at the same latitude is subtracted to remove the effects of large-scale process on SST. But SST tendency in the ocean area west of the upwelling region, dominated by the SCS western boundary advection (Liu et al., 2004), is not a good proxy for large-scale process. Thus the upstream of the upwelling where coastal upwelling does not occur (the northern tip) is chosen. In this study, SST tendency in a given month is calculated by the difference between SST in the given month and that in the previous one. The results show that SST cooling induced by coastal upwelling appears nearby the northwest corner of Borneo in December, attains maximum off the northwest coast in January with around 0.6°C cooling nearby the northwest corner of Borneo, weakens in February with 0.1–0.2°C cooling off the coast, and almost disappears near the coast in March (Fig. 5), which means that coastal upwelling forms in December, matures in January, decays in February and almost disappears in March. The month-to-month variability of the upwelling can also be observed from the WOA01 temperature tendency: coastal upwelling has a maximum depth of about 120 m and a maximum cooling of 2°C nearby Borneo in January and then it becomes shallower and weaker in February (Fig. 6).

As mentioned above, both Ekman transport induced by the alongshore winter monsoon and Ekman pumping due to the positive wind stress curl are favorable for coastal upwelling off northwest Borneo. In order to quantify the relative importance of the Ekman transport and Ekman pumping to the upwelling, the average Ekman transport and Ekman pumping are calculated from the northern tip to Kuala Belait where wind stress curl decreases sharply (Fig. 1b). Both transport estimates show similar month-to-month variability (Fig. 7): they attain maximums in January and then weaken in February, which is consistent with that of coastal upwelling. A comparison of them shows the Ekman transport is two times larger than the Ekman pumping and the Ekman transport tendency accounts for about 90% of the total transport (the sum of Ekman transport and Ekman pumping) tendency in January and February, demonstrating that the Ekman transport makes a greater contribution to the upwelling than the Ekman pumping and dominates the month-to-month variation of coastal upwelling. We also notice that Ekman transport and Ekman pumping in December and March are helpful for the upwelling, but upwelling-induced SST changes show the upwelling almost does not occur, probably because winds are weaker than the threshold value for the upwelling and cannot bring cold water from the pycnocline to the surface (Roughan et al., 2006; Taylor et al., 2008).

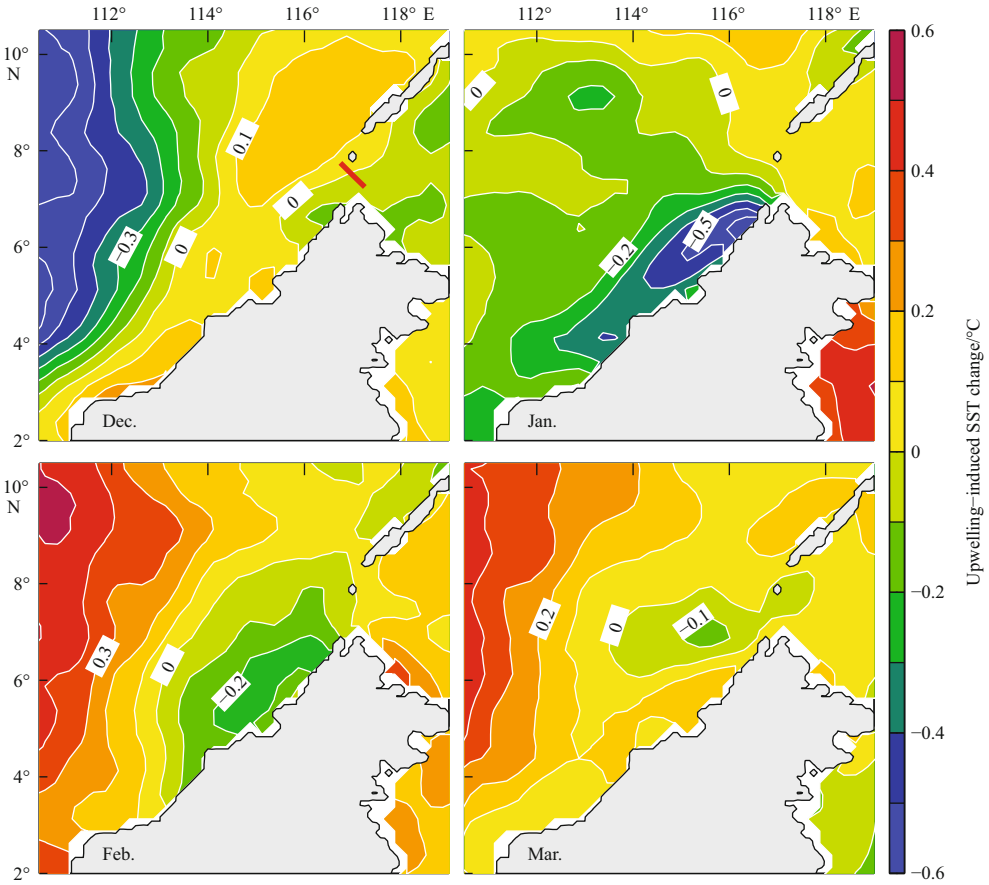

Fig. 5. Month-to-month variation of upwelling-induced changes in SST (°C). Upwelling-induced changes in SST are estimated as the difference of SST tendency and SST tendency at the northern tip (marked by red line in the upper left panel).

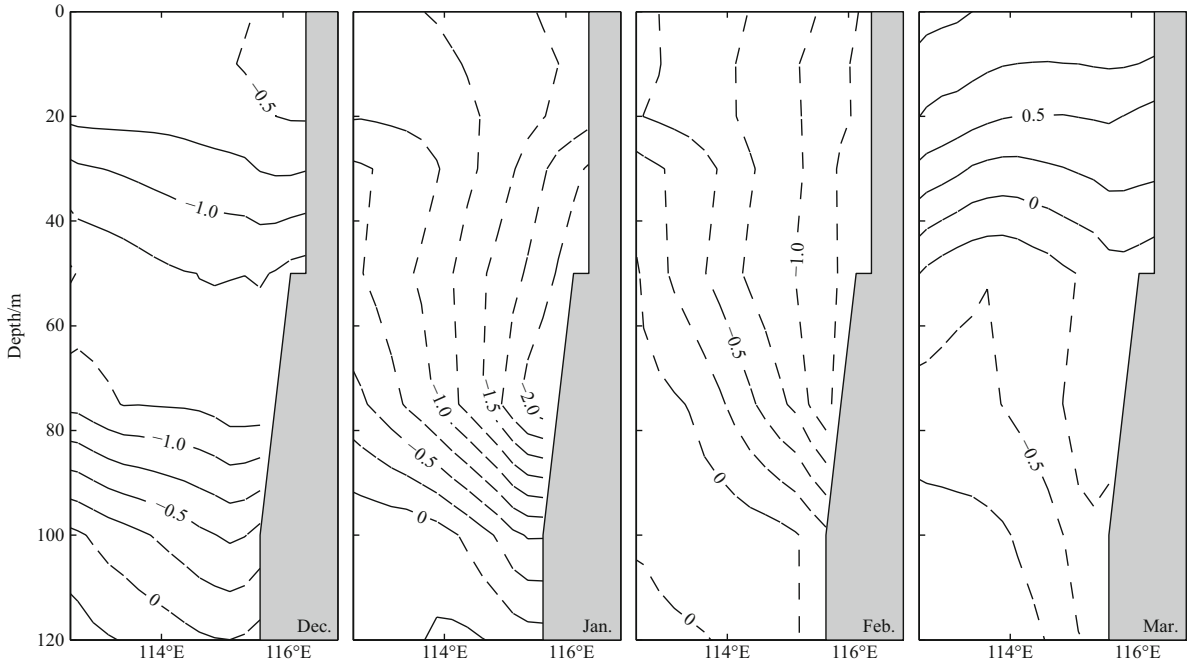

Fig. 6. Month-to-month variation of the WOA01 temperature tendency (°C) along a zonal cross section. The location of section is marked by dashed black line in Fig. 3a.

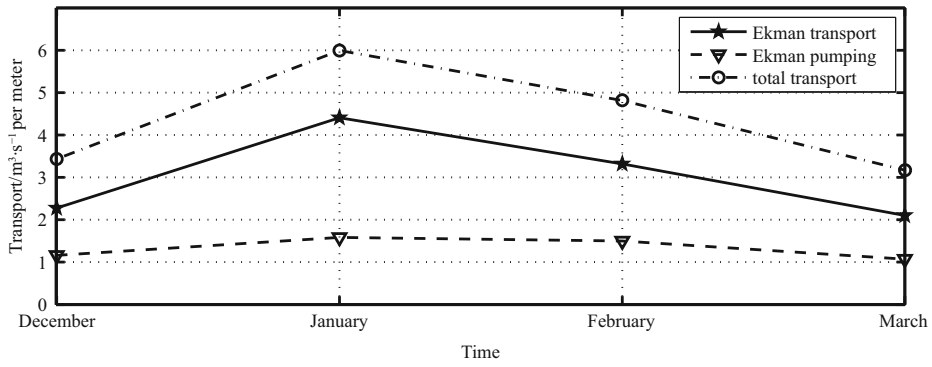

Fig. 7. Month-to-month variation of average Ekman transport (solid), Ekman pumping (dashed) and total transport (dash-dotted) calculated from the northern tip to Kuala Belait. Total transport is the sum of Ekman transport and Ekman pumping.

3.3 *Interannual variability of winter coastal upwelling*

Figure 8a shows the correlation coefficients in the SCS between winter mean SST and January Niño3.4 SST. A positive correlation occurs in most parts of the SCS, especially off southeast Vietnam. This is because cold advection by the SCS western boundary current reduces, resulting in a warming cold tongue off southeast Vietnam during winter of El Niño years (Liu et al., 2004). In contrast, a significant negative correlation is found off the northwest Borneo coast (in coastal upwelling area), indicating that winter coastal upwelling may has remarkable interannual variability associated with El Niño-Southern Oscillation (ENSO).

To examine the interannual variability of the upwelling, an upwelling index (UI) is introduced, which is estimated as winter mean SST difference between ocean and coastal area (the black line and box in Fig. 8a) at the same latitude (Nykjaer and Van Camp, 1994; Santos et al., 2005; de Castro et al., 2008). Larger UI represents stronger upwelling. The results show that UI has strong positive correlation with January Niño3.4 SST (correlation coefficient is 0.74) and winter mean Chl *a* (correlation coefficient is 0.71) (Fig. 9), which means winter coastal upwelling off northwest Borneo intensifies (reduces) during El Niño (La Niña) years, bringing more (less) nutrient-rich water and causing an increase (decrease) of Chl *a*. Due to the enhancement (weakening) of the upwelling, anomalous surface cooling (warming) occurs off the northwest Borneo coast during winter of El Niño (La Niña) years, thus a negative correlation occurs off the northwest Borneo coast. The SST anomaly (SSTA) associated with ENSO off the northwest Borneo coast has an opposite phase to that off southeast Vietnam, resulting in a SSTA seesaw pattern in the southern SCS in winter.

Previous studies have testified that the SCS monsoon has remarkable interannual variability associated with ENSO (e.g., Fang et al., 2006; Chen and Wang, 2014). During winter of El Niño years, an anticyclonic wind anomaly forms in the SCS (Fig. 8b), which is generated through atmosphere bridge (Klein et al., 1999; Wang, 2002, 2005). The anticyclonic anomaly behaves a northeasterly anomaly and a positive wind stress curl anomaly

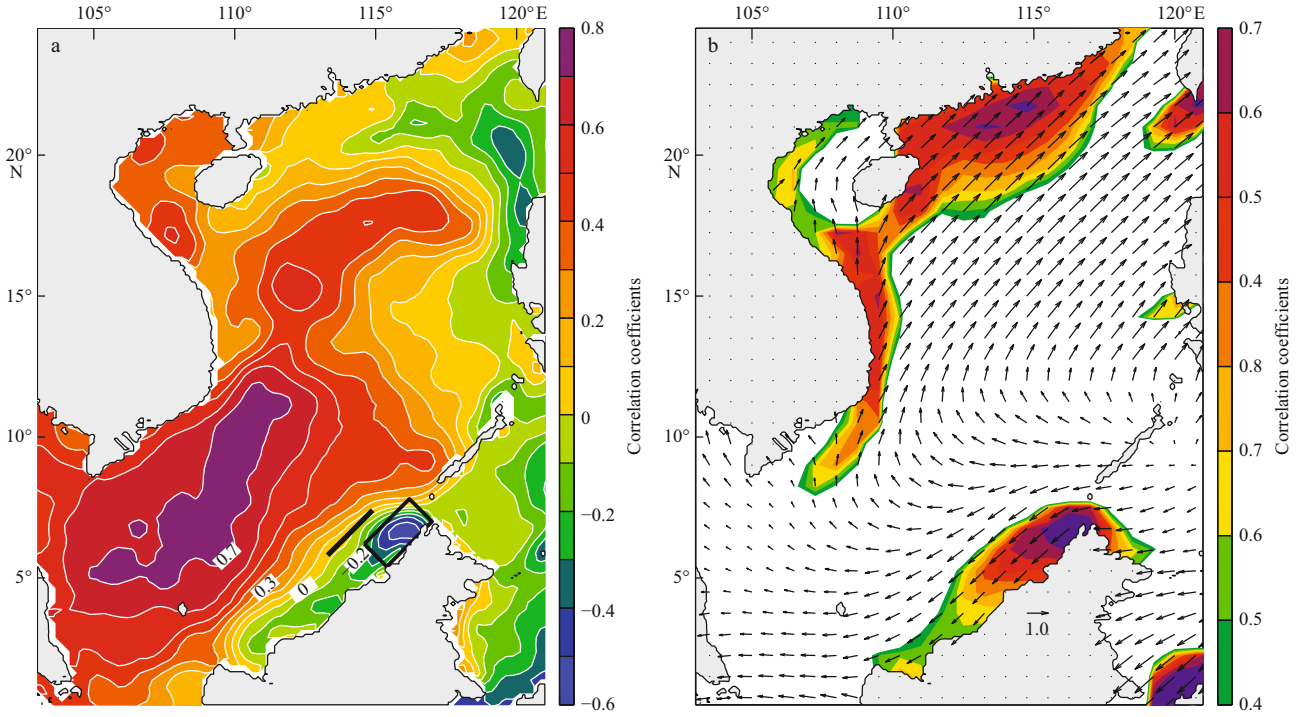

Fig. 8. Correlation coefficients in the SCS between January Niño3.4 SST and (a) winter mean SST, (b) winter mean wind vector (arrow), wind stress curl (color). Correlation coefficients larger than 0.36 are significant at the 0.05 level. Black line and box are the location of ocean and coastal area used to calculate upwelling index.

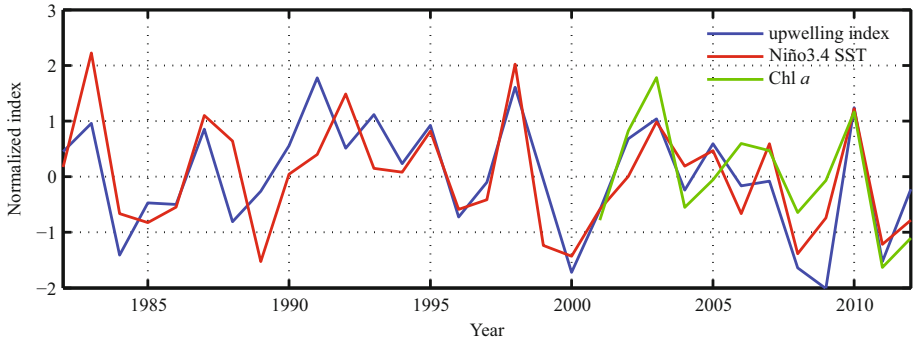

Fig. 9. Time series of upwelling index (blue), January Niño3.4 SST (red) and winter mean Chl *a* (green) normalized by their respective RMS variance (0.26°C, 1.29°C and 0.20 mg/m^3). Chl *a* is calculated in the box in Fig. 8a.

off the northwest Borneo coast (Fig. 8b). Both of them can enhance the upwelling, resulting in anomalous cooling and higher Chl *a*. The situation is reversed during winter of La Niña years.

4 Summary and discussion

Winter coastal upwelling off northwest Borneo in the SCS is investigated using satellite data, the WOA01 temperature and salinity fields and reanalysis data. Upwelling-induced changes in SST suggest that the upwelling has obvious month-to-month variation: it forms in December, matures in January, decays in February and almost disappears in March. The month-to-month variability can also be observed from the WOA01 data.

Both Ekman transport induced by the alongshore winter monsoon and Ekman pumping due to orographic wind stress curl are favorable for the upwelling. Transport estimates show that the month-to-month variability of Ekman transport and Ekman pumping are both consistent with that of winter coastal upwelling, but Ekman transport makes a greater contribution to the upwelling than Ekman pumping and determines its month-to-month variability.

Under the influence of ENSO, the upwelling shows remarkable interannual variability. During winter of El Niño (La Niña) years, an anticyclonic (a cyclonic) wind anomaly, behaving a northeasterly (southwesterly) anomaly and a positive (negative) wind stress curl anomaly off northwest Borneo, enhances (reduces) coastal upwelling, resulting in anomalous cooling (warming) and higher (lower) Chl *a*. The SSTA associated with ENSO off the northwest Borneo coast has an opposite phase to that off southeast Vietnam, resulting in a SSTA seesaw pattern in the southern SCS in winter.

The paper presents our most up-to-date information about the physical environment of winter coastal upwelling off northwest Borneo, which is of great oceanographic significance in the pursuit of understanding its effects on upwelling ecosystem

and fishery. Besides, most of previous studies on upwelling in the SCS focused on the western boundary and northern continental shelf in summer (e.g., Xie et al., 2003; Jing et al., 2011), the work fills the gap in winter coastal upwelling along the eastern boundary of the SCS to a certain extent.

References

Barth J A, Menge B A, Lubchenco J, et al. 2007. Delayed upwelling alters nearshore coastal ocean ecosystems in the northern California current. Proceedings of the National Academy of Sciences of the United States of America, 104(10): 3719–3724

Boyer T, Levitus S, Garcia H, et al. 2005. Objective analyses of annual, seasonal, and monthly temperature and salinity for the World Ocean on a 0.25 grid. International Journal of Climatology, 25(7): 931–945

Castelao R M, Barth J A. 2006. Upwelling around Cabo Frio, Brazil: The importance of wind stress curl. Geophys Res Lett, 33: L03602

Chen Changlin, Wang Guihua. 2014. Interannual variability of the eastward current in the western South China Sea associated with the summer Asian monsoon. J Geophys Res Oceans, 119: 5745–5754

Croquette M, Eldin G, Grados C, et al. 2007. On differences in satellite wind products and their effects in estimating coastal upwelling processes in the south-east Pacific. Geophys Res Lett, 34: L11608

De Castro M, Gómez-Gesteira M, Lorenzo M N, et al. 2008. Influence of atmospheric modes on coastal upwelling along the western coast of the Iberian Peninsula, 1985 to 2005. Climate Research, 36(2): 169–179

Dee D P, Uppala S M, Simmons A J, et al. 2011. The ERA-Interim reanalysis: configuration and performance of the data assimilation system. Quart J Roy Meteor Soc, 137(656): 553–597

Enriquez A G, Friehe C A. 1995. Effects of wind stress and wind stress curl variability on coastal upwelling. J Phys Oceanogr, 25(7): 1651–1671

Fang Guohong, Chen Haiying, Wei Zexun, et al. 2006. Trends and interannual variability of the South China Sea surface winds, surface height, and surface temperature in the recent decade. J Geophys Res, 111: C11S16

Isoguchi O, Kawamura H, Ku-Kassim K Y. 2005. El Niño–related offshore phytoplankton bloom events around the Spratley Islands in the South China Sea. Geophysical Research Letters, 32(21): L21603

Jing Zhiyou, Qi Yiqian, Du Yan. 2011. Upwelling in the continental shelf of northern South China Sea associated with 1997–1998 El Nino. J Geophys Res, 116: C02033

Jing Zhiyou, Qi Yiquan, Hua Zulin, et al. 2009. Numerical study on the summer upwelling system in the northern continental shelf of the South China Sea. Continental Shelf Research, 29(2): 467–478

Klein S A, Soden B J, Lau N C. 1999. Remote sea surface temperature variations during ENSO: Evidence for a tropical atmospheric bridge. Journal of Climate, 12(4): 917–932

Knee T C, Ishizaka J, Ransi V, et al. 2006. Oceanographic events at Northern Borneo and their relationship to harmful algal blooms. Scientific Paper Presented at ISRS

Liu Qinyu, Jiang Xia, Xie Shangping, et al. 2004. A gap in the Indo-Pacific warm pool over the South China Sea in boreal winter: Seasonal development and interannual variability. J Geophys Res, 109: C07012

Nykjær L, van Camp L. 1994. Seasonal and interannual variability of coastal upwelling along northwest Africa and Portugal from 1981 to 1991. Journal of Geophysical Research: Oceans (1978–2012), 99(C7): 14197–14207

Pickett M H, Paduan J D. 2003. Ekman transport and pumping in the California Current based on the US Navy's high-resolution atmospheric model (COAMPS). Journal of Geophysical Research: Oceans (1978–2012), 108(C10): doi: 10.1029/2003JC001902

Reynolds R W, Smith T M, Liu C, et al. 2007. Daily high-resolution-blended analyses for sea surface temperature. Journal of Climate, 20(22): 5473–5496

Roughan M, Garfield N, Largier J, et al. 2006. Transport and retention in an upwelling region: the role of across-shelf structure. Deep-Sea Research Part II, 53(25–26): 2931–2955

Santos A M P, Kazmin A S, Peliz A. 2005. Decadal changes in the Canary upwelling system as revealed by satellite observations: Their impact on productivity. Journal of Marine Research, 63(2): 359–379

Smith R L. 1968. Upwelling. Oceanogr Mar Biol Ann Rev, 6: 11–46

Taylor S V, Cayan D R, Graham N E, et al. 2008. Northerly surface winds over the eastern North Pacific Ocean in spring and summer. Journal of Geophysical Research, 113: D02110

Wang Chunzai. 2002. Atmospheric circulation cells associated with the El Niño-Southern Oscillation. J Climate, 15(4): 399–419

Wang Chunzai. 2005. ENSO, Atlantic climate variability, and the Walker and Hadley circulations. In: The Hadley Circulation: Present, Past and Future. Netherlands: Springer, 173–202

Wang Sufen, Tang Danling, He Fangliang, et al. 2008. Occurrences of harmful algal blooms (HABs) associated with ocean environments in the South China Sea. Hydrobiologia, 596(1): 79–93

Xie Shangping, Xie Qiang, Wang Dongxiao, et al. 2003. Summer upwelling in the South China Sea and its role in regional climate variations. J Geophys Res, 108(C8): doi: 10.1029/2003JC001867

Yao Jinglong, Belkin I, Chen Ju, et al. 2012. Thermal fronts of the southern South China Sea from satellite and in situ data. International Journal of Remote Sensing, 33(23): 7458–7468